Trehalose uptake and dehydration effects on the cryoprotection of CHO-K1 cells expressing TRET1

Tsutomu UCHIDA[a*], Maho FURUKAWA[b], Takahiro KIKAWADA[c,d],

Kenji YAMAZAKI[a], and Kazutoshi GOHARA[a]

[a] Division of Applied Physics, Faculty of Engineering, Hokkaido University, N13 W8 Kita-ku, Sapporo, Hokkaido 060-8628, Japan

[b] Division of Applied Physics, Graduate School of Engineering, Hokkaido University, N13 W8 Kita-ku, Sapporo, Hokkaido 060-8628, Japan

[c] Anhydrobiosis Research Group, Institute of Agrobiological Sciences, National Agriculture and Food Research Organization, Ohwashi 1-2, Tsukuba, Ibaraki 305-8634, Japan

[d] Graduate School of Frontier Sciences, The University of Tokyo, 5-1-5, Kashiwanoha, Kashiwa, Chiba 277-8561, Japan

* Corresponding author; e-mail: t-uchida@eng.hokudai.ac.jp; tel & fax: +81-11-706-6635

E-mail address: TU: t-uchida@eng.hokudai.ac.jp

MF: shakiiiiin0a0@gmail.com

TK: kikawada@affrc.go.jp

KY: k-yamazaki@eng.hokudai.ac.jp

KG: gohara@eng.hokudai.ac.jp

Abstract

Chinese hamster ovary cells (CHO-K1 cells) in which the trehalose transporter (TRET1) is expressed can have greater cryoprotection than ordinary CHO-K1 cells. This study examines the uptake characteristics of trehalose into cells via TRET1 and determines the influence of intracellular trehalose on the freeze–thaw viabilities. In our experiments, the intracellular trehalose concentration is controlled by the extracellular trehalose concentration and the immersion time in a freezing solution. In this freezing solution, both kinds of CHO-K1 cells are independently dispersed with various amount of trehalose, and then put into the CO_2 incubator for 0 to 6 h. After a set immersion time, the cell-suspended sample is cooled to 193 K, stored for 1 week, then quickly thawed at 310 K and its viability measured. The uptake amount of intracellular trehalose is measured before freezing. We find an upper limit for the uptake amount of trehalose when the extracellular trehalose concentration is about 400 mM, at which the freeze–thaw viability is the highest. When the extracellular trehalose concentration exceeds 400 mM, shorter immersion times are needed to obtain the maximum freeze–thaw viability. Also, longer immersion weakens the cells. Our analyses indicate that when the extracellular trehalose-concentration is less than 400 mM, the trehalose uptake occurs more slowly with less dehydration, resulting in less stress on the cell. When the extracellular trehalose concentration exceeds the saturation level, the cell is stressed by the excess dehydration due to the remaining osmotic pressure, with apoptosis occurring before freezing. (246 words)

＜Key words＞

trehalose transporter, freeze–thaw viability, immersion time, maximum uptake, apoptosis rate, optimum conditions (6 words)

<Abbreviations>

TRET1, trehalose transporter 1; Me_2SO, dimethyl sulfoxide; SD, standard deviation; CPA, cryoprotective agent; PBS, phosphate-buffered salts; HPLC, high-performance liquid

chromatography; PI, propidium iodide; 7-AAD, 7-amino-adinomycin D;

Introduction

Cell cryopreservation is an essential part of several technologies including transplantation, the screening for new drugs, and breeding in the fishing and livestock industries. The key problem in cryopreservation is finding ways to avoid intracellular freezing during the freezing, storage, and thawing processes [27, 29]. In the slow-freezing cryopreservation method, freezing outside the cells occurs preferentially during a slow temperature drop, thus dehydrating the inside of the cells and hence raising the concentration in the cytosol. This higher concentration suppresses intracellular freezing. In the vitrification method, the aim is to prevent freezing by vitrifying both the inside and the outside of the cell [12]. Each method has advantages and disadvantages, but the slow-freezing method is more useful in industry because it can cryopreserve and store a larger number of cells than the rapid-freezing method.

For both methods, a cryoprotective agent (CPA) is used as an additive to support the ice growth inhibition. An early CPA to be discovered was glycerin [35], after which cryopreservation progressed rapidly with other CPAs also being developed. Currently, dimethyl sulfoxide (Me_2SO) is often used as an effective CPA, but it is cytotoxic [19, 26, 49]. As a less toxic replacement, disaccharides such as sucrose and trehalose have been studied. Such CPAs are promising candidates because they are naturally produced as the freezing tolerances of animals [24, 32, 37] and have a strong interaction with water [13, 20, 41]. However, disaccharides are not permeable to the cell membrane due to their large molecular size, which may explain why simply adding them to the extracellular solution immediately prior to freezing has not produce a sufficient cryoprotective effect [33].

Thus various methods have been explored to introduce non-native disaccharides, such as trehalose, into mammalian cells. These methods include the invasive transportation methods such as exogenous expression of the biosynthetic enzymes [16], pore-forming molecules [9, 11, 38], activation of native channels [8], microinjection [9, 11], and electropermeabilization [40]. These

methods can greatly stress the cells. Also, they cannot easily transport trehalose into a large number of cells simultaneously. The noninvasive methods include trehalose loading using thermotropic phase transition during chilling [1], or freezing [14, 56], as well as the passive process of fluid-phase endocytosis [17, 34, 52]. These methods are useful for various cell types, but the transportation direction is one-way and the uptake amounts are relatively small.

Recently, a trehalose transporter from the anhydrobiotic larvae of the African chironomid, *Plypedilum vanderplanki,* hereafter TRET1, has been isolated and stably expressed in mammalian cells [18, 22, 30]. Those studies found that TRET1 was expressed on the cell membrane and selectively permeated trehalose. As a test of whether TRET1 plays an efficient role on CHO-K1 cells, we ran cryopreservation experiments with trehalose as a CPA, comparing CHO-K1 cells expressing TRET1 (CHO-TRET1) to cells not expressing them (CHO-vector) [47]. We found that the freeze–thaw viability of CHO-TRET1 cells under appropriate conditions was nearly 10 times that of the CHO-vector. Thus, one can drastically increase the cryoprotective effect by introducing trehalose into cells. Moreover, as this method puts less stress on cells, the maximum viability obtained in CHO-TRET1 cells was as high as those with mechanical trehalose uptake methods [9, 10, 36, 38, 40]. However, our previous study [47] also found that the cell viability decreases when the extracellular trehalose-concentration exceeds 500 mM. Chakraborty *et al.* [2] showed that the drying–condensation viability of the same CHO-TRET1 cells decreases for longer immersions in trehalose-containing media. Motivated by these previous findings, we investigate here the immersion-time dependence of the freeze–thaw viability, helping to reveal the role of intracellular-trehalose on the cryopreservation processes.

We show here that the freeze–thaw viability improves as the immersion–time increases, as long as the extracellular trehalose-concentration remains below about 400 mM. At this optimal concentration, the viability improves until the immersion time reaches about 2 hours, and after that it maintains high viability. In contrast, in a medium containing over 500 mM trehalose, and also for all conditions involving CHO-vector cells, the longer the immersion time, the lower the viability. From these findings and the direct measurement of intracellular-trehalose concentration taken during the immersion period, we argue that there is a limit to the amount of trehalose taken

into CHO-TRET1 cells. When the extracellular trehalose-concentration exceeds this limit, the cells undergo excessive dehydration and their activities decrease due to apoptosis.

Materials and methods

Cell culture and freeze–thaw experiments

In the experiments, we used the same cell cultures and a similar procedure as in our previous study [47]. As before, gene-modified Chinese hamster ovary (Flp-In™-CHO) cells were purchased from Invitrogen (Thermo Fisher Scientific, Waltham, MA, USA). TRET1 expression vector (pcDNA5/FRT-PvTret1-AcGFP1) for CHO-cell expression was prepared. To generate a stable cell line, first the TRET1 sequence was fused with a green fluorescent protein (GFP) tag at the C-terminus by subcloning into the vector. Then, stable cell lines were generated using the Flip-in system (Thermo Fisher Scientific). Briefly, intact Flp-In™-CHO cells were transfected with pcDNA5/FRT-PvTret1-AcGFP1 and pOG44 Flp-recombinase expression vector (Thermo Fisher Scientific) using Fugene6 (Roche, Basel, Switzerland). We refer to this stable line as CHO-TRET1 cells. As a negative control, the pcDNA5/FRT vector was transfected to Flp-In™-CHO cells, which is designated as CHO-vector cells.

Their culture medium was nutrient mixture F-12 Ham medium (Sigma-Aldrich, St. Louis, MO, USA) supplemented with 10% fetal bovine serum (Thermo Fisher Scientific), 1% penicillin–streptomycin (100 U/mL penicillin G and 100 mg/mL streptomycin, Thermo Fisher Scientific), 1% glutamax (100, Thermo Fisher Scientific), and 0.8% hygromycin B solution (Nacalai Tesque, Kyoto, Japan). The cell cultures were multiplied in 75-cm^2 tissue-culture flasks (AS ONE, Osaka, Japan), stored in the CO_2 incubator (MCO-18AIC, Sanyo, Osaka, Japan) at 310 K under 100% humidity, then equilibrated with a mixture of 5% CO_2 and 95% air.

When the CHO-vector and CHO-TRET1 cells reached more than 80% confluence during their cultivation, they were dissociated from the flasks by trypsinization (0.05% trypsin–EDTA solution, Thermo Fisher Scientific) and collected using a centrifuge at 1000 rpm for 3 min. Then we

prepared the cell suspension by replacing the cell-culture medium with the freezing solution, that is the cell-culture medium plus a set amount of trehalose (purity 99.9%, endotoxin free, donated by Hayashibara). The extracellular trehalose concentration C_0 in this freezing solution ranged within 0 – 1000 mM (C_0 and all other symbols are defined in Table 1). Then, one milliliter of the cell suspension (of the other 10^5 – 10^6 cells/mL) was put into a 1.8-mL cryotube vial (Thermo Fischer Scientific). To investigate the immersion-time dependence on the freeze–thaw viabilities, six cell-suspension samples for one experimental condition were prepared and stored in the CO_2 incubator for the time periods of 0, 0.5, 1, 2, and 4 h. For testing C_0 dependence on the freeze–thaw viabilities, the freezing temperature was set at T = 198 K. At this condition, the cooling rate was about 10 K/min. To instead test the setting-temperature dependence, we fixed C_0 at 500 mM.

Since the cryopreserved cells at T = 198 K exhibit stable freeze-thaw viabilities at least for one year [48], we only investigated sample storage for a week, the same period we used before [47]. After being stored for a week, the individual vials were thawed in a water bath at 310-K until all extracellular ice melted (about 5 min). During this process, the temperature increased by about 50 K/min. The freezing solution in the thawed-cell suspension was then rinsed with the culture medium twice. Since TRET1 transports trehalose in both directions [22], this rinsing removes most of the trehalose (both extra- and intracellular).

The freeze–thaw viability of CHO-K1 cells (η^F) were obtained from their fluorescence images with a cell-stain kit (Dojindo, Kumamoto, Japan). This kit includes calcein-AM (acetoxymethylated calcein) and PI (propidium iodide) solutions, with the procedure using an epifluorescence microscope (IX71; Olympus) through an Olympus LCPLFL 20× objective lens attached to a charge-coupled device camera (DP70; Olympus). To obtain the average viability, we used the number ratio of living cells to the total number of cells in eight fluorescence images taken from one sample. To this data, we added viability data for 6-h immersion from our previous study [47].

To estimate the accuracy of the viability, we repeated the freeze–thaw tests at least three times for one experimental condition with the independent cell lines. The resulting viability here was the average for the indicated experimental conditions ± the standard deviation (SD) of all

111 measured data. The cells displaying no color with the stain kit were treated as measurement
112 uncertainty. Here, this uncertainty was found to be much less than the SD value. For statistical
113 analysis, data were analyzed using two-way ANOVA with a Tukey–Kramer post-hoc test (Microsoft
114 Excel 2010 and BellCurve for Excel) for at least 99% confidence.
115 After thawing, the growth efficiency of the surviving cells was also checked by plating the
116 cells in a 24-well cell-culture plate (Nippon Genetics, Tokyo, Japan). The plated cells were incubated
117 in a CO_2 incubator for at most one week and their adhesion–proliferation processes were observed
118 with a microscope (IX71; Olympus). Further details of the complete procedure are in reference [47].
119
120 *Apoptosis assay of CHO-K1 cells during the immersion period*
121
122 Before freezing, CHO-K1 cells were immersed in the freezing solution with trehalose to
123 take trehalose into cells. However, the trehalose may stress the cells via osmotic pressure, thus
124 weakening the cells. To account for this effect on the freeze–thaw viability, we measured the
125 apoptosis ratio of CHO-K1 cells via a flow cytometry (Muse™ cell analyzer; Merck) with a double
126 stain (Annexin V & dead cell kit; Merck) consisting of annexin-V (a calcium-dependent
127 phospholipid-binding protein with high affinity for phosphatidylserine) and 7-amino-adinomycin D
128 (7-AAD) nuclear staining dye. The 1 mL of cell suspension was immersed in the freezing solution
129 with trehalose at C_0 = 0, 100, 250, 500, and 750 mM, and then stored in the CO_2 incubator for up to
130 6 h. Five samples prepared in the same C_0 condition were incubated simultaneously, and then one of
131 them was picked up for measuring the apoptosis ratio at a given immersion time (0.5, 1, 2, 4, and 6
132 h).
133
134 *Trehalose uptake assay of TRET1 proteins in CHO-K1 cells*
135
136 The amount of trehalose taken into the CHO-K1 cells was directly measured on both
137 CHO-TRET1 and CHO-vector cells. In both cases, the cell suspension had between 10^6 and 10^7
138 cells/mL that were incubated at 310 K for different time periods (from 0.5 to 6 h) in the freezing

solution containing trehalose of C_0 from 100 to 1000 mM. Then an extracted sample was rinsed with phosphate-buffered salts (PBS) three times and replaced with 0.5 mL ethanol including 0.1 mg of sorbitol as the reference. Then we ran high-performance liquid chromatography analysis (HPLC: LC-10A system, Shimadzu). Further details of this measurement are in Watanabe *et al.* [50].

Results

Freeze–thaw viability: dependence on immersion time

The freeze–thaw viabilities of CHO-vector cells η^F_V and CHO-TRET1 cells η^F_T incubated for immersion time t with extracellular trehalose concentration C_0 are shown in Fig. 1. When C_0 is 0 or 100 mM (Fig. 1(a)), both η^F_V and η^F_T are relatively low for all t. In contrast, when $C_0 = 250$ mM, both η^F_V and η^F_T are significantly higher, showing clear trends with t. In particular, η^F_V gradually decreases with t, whereas η^F_T increases, showing significantly larger values than η^F_V ($p < 0.01$). These results indicate that the trehalose acts as a CPA at $C_0 > 100$ mM, and that the viability of CHO-K1 is improved by the uptake of trehalose into the cell.

The higher concentrations in Figs. 1(b) and (c) show more distinct trends. For the intermediate concentrations of 300 and 400 mM, the CHO-TRET1 value η^F_T at $t = 0$ h is larger than that at the lowest concentration conditions. Then they gradually increase with t, and level off at $t >$ 2 h with a value of about 0.8 for 400 mM (Fig. 1(b)). Conversely, for the CHO-vector cells at $C_0 = 300$ and 400 mM, η^F_V decreases with t, similar to that observed at 250 mM. At the highest concentrations, $C_0 \geq 500$ mM (Fig. 1(c)), both η^F_V and η^F_T at $t = 0$ h are as high as those for $C_0 = 300$ and 400 mM. But for η^F_T, the trends with t differ, showing maximum viabilities at $t = 2$ h and 0.5 h for 500 and 1000 mM, respectively. At longer immersion times, they decrease with t. Conversely, η^F_V in 500 mM and 1 M decrease monotonically with t. Overall, the results show that the highest, and most steady, viabilities are obtained with CHO-TRET1 immersed in the extracellular medium of about 400 mM for a time $t > 2$ h. This optimum concentration of the extracellular trehalose coincides well with that obtained in our previous study [47].

Concerning the cryopreservation of CHO-vector cells, these results show that η^{F}_{V} at $t = 0$ h is higher for higher C_0. This trend means that the extracellular trehalose acts as a CPA for CHO-vector cells. However, η^{F}_{V} gradual decreased with t at all C_0 values. Thus, a high extracellular concentration of trehalose is relatively toxic to the CHO-vector cells. We also found that η^{F}_{V} was very small, which was similar to η^{F}_{T} when C_0 was less than 100 mM. This means that when $C_0 \leq$ 100 mM, extracellular trehalose does not work as a CPA for either CHO-K1 or CHO-TRET1 cells.

Observing the cryopreserved cells with a microscope after thawing, we found that the survived cells after thawing adhered and proliferated as also seen on the normally cultivated cells (data not shown). This observation agreed with our previous study [47]. Thus, the freeze-thaw viabilities obtained by the membrane integrity assay are also valid for their healthiness.

Apoptosis of CHO-K1 cells during immersion in the freezing solution

We now examine why both η^{F}_{V} and η^{F}_{T} varied with the immersion time t. A possible reason is apoptosis of CHO-K1 cells before freezing. To test this mechanism, we co-stained the cells with annexin-V and 7-AAD during their immersion for 0.5 to 6 h in the freezing solution. The extracellular trehalose concentration C_0 in the medium varied from 0 to 750 mM. We distinguish the apoptotic ratio A as early apoptosis A^E and late apoptosis A^L. With A^E, the annexin-V is positive and the 7-AAD negative, whereas for A^L, both measures are positive.

The results in Fig. 2 show that the apoptosis occurred during immersion under all conditions. Even at $C_0 = 0$ mM (the normal culture medium), both A^{E}_{V} and A^{E}_{T} exceed 0.1 at $t = 6$ h, which is significant compared to the measurement errors. The apoptosis of both CHO-K1 cells in a cryotube with the culture medium may arise from either anoxia or poor nutrition due to the suspended state having a high number density (10^5–10^6 cells/mL) over a long time. This result indicates that about 10% of the viabilities obtained in the previous section are caused by apoptosis of the cells before freezing, and thus the actual viabilities after the freeze–thaw process should be higher than those shown in Figs. 1(a)–(c).

At $C_0 = 100$ mM, apoptotic ratios of CHO-TRET1 and CHO-vector cells are almost the same

as those of C_0 = 0 mM (Fig. 2). Thus, when C_0 is small enough to show no significant CPA effect, both CHO-K1 cells also show no effect of apoptosis of during immersion. This lack of effect applies to both extracellular and intracellular trehalose.

Referring to the results in Fig. 2, $A^E > A^L$ for all cases except C_0 = 500 mM and $t > 0.5$ hr. Also, for both CHO-K1 cells, both $A^E{}_V$ and $A^E{}_T$ tend to increase with C_0 and t. Also, $A^E{}_V$ is usually larger than $A^E{}_T$. When $C_0 > 500$ mM and $t > 2$ h, the value of A^L increases with increasing C_0 and t. This increase is larger for CHO-vector cells than for CHO-TRET1 cells. Consequently, the effect of apoptosis during the immersion period should strongly affect their freeze–thaw viabilities for larger C_0 and longer t conditions.

Consider now the reason for this apoptosis. Given that 1) the apoptotic ratios increased with C_0 and t when trehalose was added, but 2), the ratios were lower in CHO-TRET1 cells than in CHO-vector cells, then we suggest that the cell unhealthiness during immersion arises from excessive dehydration in the cells. Such an effect likely arises from osmosis driven by the trehalose concentration difference across the cell membrane. This is supported by optical microscopy of CHO-K1 cells during the immersion period (see Appendix).

To estimate the effect of the extracellular trehalose-concentration on the apoptotic ratio, we examine the rate of increase of apoptosis. Consider a simple exponential fit of A with immersion time t:

$$A = A^E + A^L = A_0 \exp(K^A t), \quad (1)$$

where A_0 is a constant and K^A is the time constant of the apoptotic rate. We estimated K^A for both CHO-vector cells $K^A{}_V$ and CHO-TRET1 cells $K^A{}_T$ for different C_0. Figure 3 shows that the apoptotic rates of both kinds of cells are larger at higher C_0. Also, $K^A{}_V$ is larger than $K^A{}_T$ when $C_0 < 400$ mM, but they are approximately equal at higher C_0. Thus, similar to the case of CHO-vector cells, CHO-TRET1 cells are affected by trehalose osmotic pressure when $C_0 \geq 500$ mM. The result indicates that at long immersion times the cells may be weakened by either excessive dehydration or the osmotic shock of the extracellular trehalose. This extracellular-trehalose effect is larger in

CHO-vector cells than that in CHO-TRET1 cells. As A^L increases with C_0 and t, the apoptosis should severely affect the freeze–thaw viability under such conditions.

Trehalose uptake measurements on CHO-K1 cells

The freeze–thaw viability measurements here indicate an upper limit to the uptake of trehalose into CHO-TRET1 cells. As an additional test, we used HPLC to directly measure the amount of trehalose taken into the CHO-K1 cells. The results in Fig. 4(a) show that the amount of trehalose in CHO-vector cells M_V is about 20 pg/cell or less with most conditions. Moreover, the uptake does not significantly increase with immersion time. This result suggests that the trehalose is mostly impermeable for these cells, which is consistent with the previous results [2, 22]. On the other hand, in Fig. 4(b) the uptake amount of trehalose in CHO-TRET1 cells M_T increases with t for all C_0 values except 100 mM. Moreover, the rate of increase is roughly independent of C_0 when $t \leq 2$ h. But at longer times, the uptake decreases. For $C_0 = 400$ mM, M_T continues to increase for a longer time, reaching a maximum at 80 pg/cell when $t = 4$ h before decreasing. This trend is consistent with the t dependence of η^{FT}. Therefore, the η^{FT} is higher when the uptake amount of trehalose is larger.

In the previous section, we found that $C_0 > 100$ mM was required for trehalose to function as a CPA. Using the results here, we estimate that 20 pg/cell is about the minimum trehalose uptake into CHO-K1 cells to work as a CPA. This value is equivalent to 62 fmol/cell, which is within the same order of magnitude of the 14 fmol/cell estimated by extrapolating the Michaelis–Menten coefficients [47].

Consider now the upper limit of the amount of trehalose taken into CHO-TRET1 cells. If we assume that the effective volume of a CHO-K1 cell as 488 μm^3 [2], then this maximum uptake of about 70–80 pg/cell is equivalent to about 400–500 mM, assuming an. Considering the uncertainties in the estimate, this value agrees well with the extracellular trehalose concentration. Therefore, given our earlier finding that η^{FT} saturates near $C_0 = 400$ mM, the trehalose concentration appears to be nearly in balance inside and outside the cell at the upper limit of

trehalose uptake.

However, we also found that M_T decreased at all concentrations as the immersion time increased past 2 h. Considering that the apoptotic ratio A^L increased with the immersion time, M_T might be underestimated at longer immersion times due to a decrease in cell healthiness. This effect may work as follows. As the immersion period becomes longer, the late apoptotic ratio increases, and the healthiness of the cell membrane decreases. Under such conditions, trehalose taken into the CHO-TRET1 cell may also leak out of the cell. Then, as the amount of trehalose that leaked before the HPLC measurement is removed during the rinsing process, M_T may be underestimated when normalized by the initial number of cells.

Discussion

We examined the freeze–thaw viabilities of both CHO-TRET1 and CHO-vector cells, varying the immersion time up to 6 h and trehalose concentrations up to 1000 mM. The CHO-vector cell had a higher viability in a high extracellular concentration at an immersion time of 0 h, with the value monotonously decreasing at longer immersion times. As trehalose uptake was low ($M_V <$ 20 pg/cell for most conditions), the freeze–thaw viability η^F_V appears to be controlled by the CPA effect of extracellular trehalose.

For CHO-TRET1 cells, the trehalose uptake reached a maximum (M_T; about 80 pg/cell) with $C_0 \approx 400$ mM for an immersion time near 4 h, with maximum viability $\eta^F_T \approx 0.8$. Thereafter, the viability was independent of the immersion time, indicating the uptake had reached equilibrium. When the extracellular concentration of trehalose was lower than this optimum condition, the equilibrium state was not reached even at the immersion time of 6 h, with η^F_T increasing with immersion time. In the opposite case, when the extracellular trehalose-concentration was higher than the optimum condition, the highest η^F_T value occurred for an immersion time shorter than 2 h, and thereafter η^F_T decreased with the immersion time. The uptake amount of trehalose did not exceed 80 pg/cell even when $C_0 >$ 400 mM. These findings and the apoptotic measurements during immersion indicate that the main reason for smaller viabilities

279 at higher C_0 and longer immersion times is apoptosis of the cells before freezing.

280 In addition, we found that $C_0 > 100$ mM was necessary for extracellular trehalose to behave
281 as a CPA. When the extracellular concentration was too small to express CPA behavior, the amount
282 of trehalose taken into a CHO-TRET1 cell was nearly that of a CHO-vector cell, and the apoptosis
283 during immersion was as small as the background value. Thus, at such low concentrations, the
284 uptake of trehalose into CHO-TRET1 cells is too small to act as a CPA, and the extracellular
285 trehalose cannot exhibit sufficient cryopreservation effect on both types of CHO-K1 cells.

286 When comparing the freeze–thaw viabilities of these cells with the amount of intracellular
287 trehalose, we confirmed that the optimum condition occurred at the upper limit to the uptake
288 amount of trehalose. If the extracellular trehalose concentration is below or above this value, the
289 freeze–thaw viability became lower. Based on these results, we next discuss the cryoprotection
290 mechanism of both extra- and intra-cellular trehalose.

291

292 ***Freeze–thaw viabilities of CHO-vector cells and their apoptotic conditions during immersion***

293

294 At the shortest immersion times, the osmotic effect of the extracellular trehalose on the
295 healthiness of CHO-K1 cells was very small. Even for CHO-TRET1 cells under short immersion
296 times, the extracellular trehalose was hardly taken into cells. Thus, the freeze–thaw viabilities of
297 both kinds of cells at short immersion times should be controlled by the CPA effect of the
298 extracellular trehalose. When we plot the C_0 dependence of η^{FV} and η^{FT} at $t \approx 0$, as in Fig. 5, we see
299 that η^{FV} and η^{FT} are close and have the same trend, that is, a higher freeze–thaw viability at higher
300 C_0 conditions independent on the trehalose uptake. This trend indicates that the CPA effect by
301 extracellular trehalose is expected to be higher at higher trehalose concentrations. Such an effect
302 appears consistent with several proposed cryoprotective mechanisms from extracellular trehalose:
303 (i) The trehalose induces vitrification of the extracellular solution [3, 53-55]. (ii) The trehalose
304 inhibits growth of extracellular ice crystals as well as reducing the amount of intracellular water,
305 both of which inhibits intracellular freezing [15, 44-46]. And (iii), trehalose interacts directly with
306 cell membranes and proteins and protecting them [5-6, 25, 31, 40, 42-43]. We now examine the first

two of these mechanisms in a little more detail.

Consider the vitrification mechanism (i). The temperature of 193 K is below 243 K, the glass transition temperature of the maximum freeze concentrated solution [3], but the cooling rate was too small to induce vitrification, at least of nearly pure water. As the maximum freeze concentration of trehalose is about 20 wt% [3], which is equivalent to about 600 mM, the lower concentration conditions in this study probably did not vitrify to a sufficient extent to preserve the cells. In addition, our previous study indicated that small ice crystals form in the same concentration range of the present study [44, 48]. Thus, this cryopreserving mechanism seems unlikely to have operated here.

Concerning the inhibiting extracellular ice growth mechanism (ii), an intermolecular network of trehalose in the solution should occur when the concentration exceeds 10 wt%, or about 250 mM [45-46]. Figure 5 shows that the freeze–thaw viability is high at this and higher concentrations. At concentrations below 200 mM (≈ 6 wt%), the viability is low, and the viscosity of the trehalose solution is close to that of pure water [45-46]. Thus, it is considered that the trehalose cannot sufficiently inhibit the water-network construction during freezing below 200 mM. Thus, the concentration dependence is consistent with a cryoprotective mechanism involving suppression of ice crystal growth due to formation of a trehalose network in the solution.

We now examine the influence of dehydration on the CHO-vector cells caused by the extracellular trehalose. When $C_0 \geq 250$ mM, η^{FV} decreases monotonically with t (Fig. 1). This result may be due to excessive dehydration of the cells arising from osmotic pressure before freezing. This mechanism is consistent with the apoptosis ratio increasing as the viability decreases (Fig. 2), and also with the size of the cells shrinking with t (Fig. S2). To examine this mechanism, we estimate how much the intracellular water can leave via the osmotic pressure of extracellular trehalose. We now assume that the inside and outside of the cell are isotonic before adding trehalose, and the osmotic pressure Π_0 is equal to about 300 m osmol/kg [21, 39]. Then, Π_0 can be written

$$\Pi_0 = C_{out} R T = \frac{n_{in} R T}{V_0}, \quad (2)$$

where C_{out} = 154 mM is the assumed initial concentration of the extracellular matrix (equivalent to that of 0.9% NaCl solution, or of saline water), n_{in} is the initial solute concentration in the cell, V_0 = 487.59 μm^3 is the effective volume of a CHO-K1 cell [2], R = 8.31 J/mol K is the gas constant, and temperature T is set at 310 K. If we add trehalose at the concentration of C_0 into the extracellular matrix, the extracellular osmotic pressure Π_{out} becomes

$$\Pi_{out} = (C_{out} + C_0)\,RT. \quad (3)$$

To become isotonic, the cell volume will shrink by δV, making the intracellular osmotic pressure Π_{in}

$$\Pi_{in} = \frac{n_{in}RT}{V_0 - \delta V}. \quad (4)$$

Then, by setting $\Pi_{in} = \Pi_{out}$,

$$\frac{\delta V}{V_0} = \frac{C_0}{C_0 + C_{out}}. \quad (5)$$

This indicates that the dehydration rate $\delta V/V_0$ should be larger for larger C_0. We find that this $\delta V/V_0$ correlates well with the cell viability before freezing, which is defined as $\eta^A = 1 - A_{(t=6)}$, the latter variable being the apoptosis ratio A at t = 6 h (from Fig. S3, $R^2 \sim 0.84$). Here we assume that the isotonic condition was reached by 6 h, the longest immersion time. That η^{FV} monotonously decreases with t indicates that the cell was damaged by a combination of stresses, specifically, freezing, thawing, and osmotic stress by extracellular trehalose during the immersion period.

To help examine these stresses further, we model the time dependence of the viability. Here, η^{FV} is fit by the following exponential function with time constant K^{FV}:

$$\eta^{FV} = \eta^{FV0} \exp(-K^{FV} t), \quad (6)$$

where η^{F}_{V0} is a constant. After fitting the data to obtain K^{F}_{V} at various C_0, we compare them to the K^{A}_{V} values obtained earlier (from Fig. 3). The results are shown in Fig. 6. The trend shows K^{F}_{V} roughly increasing linearly for C_0 below 400 mM, then leveling off. This trend agrees qualitatively with that of K^{A}_{V}. The comparison indicates that at the lower concentrations, the stresses affecting η^{F}_{V} are dominated by the freeze–thaw process (that is, a low expression of CPA function of extracellular trehalose) rather than the influence of apoptosis. At higher concentrations, the osmotic stress dominates before freezing.

Trehalose uptake and dehydration in CHO-TRET1 cells

We now use a model to estimate the relation between the trehalose uptake into CHO-TRET1 cells and their dehydration. Extracellular trehalose is transported into CHO-TRET1 cells, driven by the concentration gradient of trehalose across TRET1 [22]. This uptake continues until the intracellular trehalose concentration equals the extracellular concentration C_0. To help us examine the inflow of trehalose and the outflow of water from the cells, the volume of cells is fixed at V_0. We also assume that the extracellular trehalose concentration C_0 remains unchanged even if trehalose flows into the cell, a reasonable assumption given that the intracellular volume is much less than that of the extracellular solution volume. Then, assuming no limit for the uptake amount, the virtual equilibrium intracellular-trehalose m_{in} is obtained from

$$C_0[mol/L] = \frac{m_{in}[g/cell]}{324.3[g/mol]\times V_0[L/cell]} \quad . \tag{7}$$

Using the model assumed in the previous section, the dehydration amount δV due to the osmotic pressure difference is

$$\delta V = \frac{C_{out}}{(C_0 - C_{in}) + C_{out}} V_0 \quad . \tag{8}$$

In this equation, the concentration difference is $C_0 - C_{in}$, where C_{in} is the intracellular trehalose

concentration, because trehalose is also taken into CHO-TRET1 cells. The measured maximum amount of trehalose taken into the cell at each concentration is C_{in}.

For $C_0 \leq 400$ mM, we find that $C_{in} \approx m_{in}$ and $\delta V \approx 0$ (Fig. 7). These results suggest that the cells are hardly dehydrated under these C_0 conditions, and also that the isotonic condition is kept mainly by the trehalose uptake. Results from optical microscopy (Figs. S1, S2) also show that, within this immersion time range, the size of CHO-TRET1 cells within this immersion time range tended to increase with time. This trend is the same as that found with 0 mM. As the same $\delta V \approx 0$ result occurs with the 0 mM case, the CHO-TRET1 cells under $C_0 \leq 400$ mM must also be keeping their healthiness during immersion. In addition, as the time constant $K^{A}{}_{T}$ for apoptosis of the CHO-TRET1 cells is smaller than that of the CHO-vector cells in this concentration range (Fig. 3), these conditions put less stress on CHO-TRET1 cells throughout the cryopreservation process.

On the other hand, when $C_0 \geq 500$ mM, C_{in} is significantly smaller than m_{in}. This deviation from m_{in} correlates well with an increase in δV (Fig. 7). This finding suggests that trehalose is taken into CHO-TRET1 cells at the same time that the cells dehydrate. Although the optical microscopy (Figs. S1 and S2) did not show significant shrinkage observed in the CHO-vector cells affected by dehydration, the apoptosis ratio of CHO-TRET1 cells A_T (or $A^{L}{}_{T}$) increased with t. This trend is similar to those observed for CHO-vector cells (Fig. 2). Therefore, under these high C_0 conditions, the CHO-TRET1 cells appear to have been highly stressed as they took in extracellular trehalose. As TRET1 is a high-capacity transporter of trehalose [22], larger C_0 should have faster saturation. This behavior is consistent with our findings in Fig. 1(c). After saturation, further immersion would lead to cell apoptosis due to excess dehydration from the remaining concentration gradient, which then causes an inability to withstand the following freezing and thawing stresses.

These analyses lead us to conclude that the uptake amount of trehalose to CHO-TRET1 cells has an upper limit value of C_{in} = 70–80 pg/cell, a value corresponding to an extracellular concentration C_0 = 400–500 mM. The value indicates that TRET1 enables a higher intracellular trehalose concentration than those obtained by other trehalose-introducing methods, including both invasive and noninvasive techniques, as well as higher freeze–thaw viabilities with less stress on the cells. Such a result may arise from the unique properties of TRET1 as a high-capacity,

418 bi-directional transporter of trehalose [22]. As shown in Fig. 7, CHO-TRET1 cells were nealy
419 isotonic by the uptake of trehalose into the cell without dehydration stress at $C_0 \leq 400$ mM, and
420 approached isotonic conditions via dehydration at $C_0 \geq 500$ mM. The transport and dehydration
421 processes should reduce the osmotic stresses on the cells, leading to relatively high viabilities.
422
423 *Uptake rate of trehalose into CHO-TRET1 cells*
424
425 As argued in the previous section, the trehalose influx gradually approaches the saturation
426 value at $C_0 \leq 400$ mM. However, the intracellular trehalose saturates in a short time at $C_0 \geq 500$
427 mM, followed by excess dehydration. Here, we estimate the trehalose uptake rate using a model of
428 trehalose diffusion through TRET1.
429 We approximate a CHO-TRET1 cell as a sphere of radius a, with a = 5.5 μm [2]. The
430 extracellular trehalose concentration C_0 is assumed constant as argued above. Assuming that the
431 initial intracellular trehalose concentration C_{in0} is 0 mM, the trehalose inflow $M_T(t)$ at time t is
432 expressed by [4]
433
434 $$\frac{M_T(t)}{M_T(\infty)} = 1 - \frac{6}{\pi^2}\sum_{n=1}^{\infty}\frac{1}{n^2} exp\left(-\frac{Dn^2\pi^2}{a^2}t\right) \quad , \qquad (9)$$
435
436 where $M_T(\infty)$ = 80 pg/cell is the intracellular trehalose content at equilibrium and D is the diffusion
437 constant. For simplicity, we just use the first term n = 1, obtaining the following solution:
438
439 $$ln\left(1 - \frac{M_T(t)}{M_T(\infty)}\right) = ln\frac{6}{\pi^2} - \frac{\Lambda\pi^2}{a^2}t \quad , \qquad (10)$$
440
441 where D has been replaced with the apparent transport efficiency Λ [m²/s]. (The reason for this
442 replacement is that trehalose transport in TRET1 may depend on the concentration gradient, which
443 is not a standard property of D.) Then, we apply Eq. (10) to the trehalose uptake data after reaching
444 the maximum (Fig. 4(b), $t \geq 2$ h) to obtain Λ for each C_0 condition. Within the concentration ranges

here, the resulting transport efficiency is of order 10^{-12} m²/s. This is two orders of magnitude smaller than the self-diffusion coefficient of water in an aqueous solution of trehalose (5.08×10^{-10} m²/s at 298 K [23]). But it is close to the diffusion coefficient of trehalose in a high-concentration aqueous trehalose solution (e.g., about 1×10^{-12} m²/s at C_0 = 71 wt% ≈ 7.5 M [7]). Therefore, this model indicates that trehalose diffuses through TRET1 at a rate comparable to that in a high-concentration aqueous solution.

The specific dependence of Λ on C_0 is a nearly linear increase with C_0 (Fig. 8, $R^2 = 0.97$). That is, the trehalose uptake rate into CHO-TRET1 cells increases with the trehalose gradient across TRET1, shortening the time to reach the upper limit of intracellular trehalose content. This is consistent with the fact that the peak of freeze–thaw viability shifts to smaller t at $C_0 \geq 500$ mM (Fig. 1). As the uptake rate of trehalose is large when $C_0 \geq 500$ mM, the intracellular concentration reaches its upper limit within 2 h of immersion. Thus, the intracellular trehalose concentration is always lower than the extracellular concentration after that time, and the cell continues to receive osmotic stress. Therefore, as results in Fig. 7 indicate, even CHO-TRET1 cells would be weakened by the excess dehydration during an overly long immersion period under these high C_0 conditions.

To test the validity of the above hypothesis, we now estimate the effect of dehydration on the freeze–thaw viability. As shown in Fig. 1c, η^{F_T} reaches a maximum value at t = 2 h at C_0 = 500 mM and at t = 0.5 h at C_0 = 1000 mM, so we consider that the CHO-TRET1 cells experience a similar dehydration situation as that of the CHO-vector cells when $t \geq 2$ h at C_0 = 500 mM and $t \geq 0.5$ h at C_0 = 1000 mM. When we examine the t dependence of η^{F_T} in these regions, we find that η^{F_T} decreases exponentially with t (Fig. 1c). We estimated the time constant K^{F_T} for each condition by fitting to Eq. (6) for the CHO-vector cells as follows, finding

$$\eta^{F_T(C_0=500)} = 0.89 \exp(-0.054\, t) \qquad t \geq 2 \text{ h } (R^2 = 0.98)$$

$$\eta^{F_T(C_0=1000)} = 0.73 \exp(-0.445\, t) \qquad t \geq 0.5 \text{ h } (R^2 = 0.99).$$

These results show that K^{F_T} = 0.054 for C_0 = 500 mM (where $C_0 - C_{in}$ = 100 mM), which is close to

473 the result $K^{F}_{V} = 0.023$ for $C_0 = 100$ mM of CHO-vector cell. Also, the value $K^{F}_{T} = 0.445$ for $C_0 = 1000$
474 mM (where $C_0 - C_{in} = 600$ mM) is close to the value $K^{F}_{V} \approx 0.58$ for $C_0 \geq 400$ mM (Fig. 6). Therefore,
475 the results can be explained with the hypothesis that the viabilities are lowered due to the extra
476 concentration of the experimental extracellular concentration over the saturated intracellular
477 concentration. If true, then the decrease in η^{F}_{T} at $C_0 \geq 500$ mM was caused mainly by cell apoptosis
478 in the immersion period. If trehalose is added to the medium in excess, trehalose above the upper
479 limit is not taken into the cell, but rather weakens the cell due to excess dehydration.
480 To reduce the risk from osmotic stress at the large trehalose-concentration differences, one
481 might try adding the trehalose to the extracellular solution in multi-steps instead of the single-step
482 method we used. In follow-up studies, we will try this and other changes to the method to help find
483 a better cryopreservation protocol.
484
485 *Re-examining of viabilities with optimal immersion time*
486
487 We have found here that the optimum immersion time for CHO-TRET1 cells is about 2 h.
488 Our previous study [47] instead used a 6-h immersion time. We now compare the older results to
489 those in the present study.
490 Consider the CHO-vector cells first. When $C_0 \geq 250$ mM, the viabilities are improved by
491 using the shorter (2 h) immersion time (Fig. 9(a)). This improvement confirms that the extracellular
492 trehalose acts as a CPA when $C_0 \geq 250$ mM. Above 400 mM, the viabilities in the 2 h case hardly
493 change (values of 0.2–0.3). This constancy is consistent with our finding that the apoptosis ratio is
494 roughly independent of C_0 when $t = 2$ h (Fig. 2(a)). Therefore, the comparison of immersion times
495 supports our proposed mechanism for the C_0 dependence of η^{F}_{V}.
496 For the CHO-TRET1 cells, the same trends occur, but are more distinct (Fig. 9(b)). In
497 addition, the concentration at which the two immersion-time cases diverge is near 400–500 mM.
498 This diversion point is a higher C_0 than that for CHO-vector. That is, the viabilities are roughly
499 consistent when $C_0 < 500$ mM, and the maximum viabilities of both immersion times are $\eta^{F}_{T} \approx 0.8$
500 at $C_0 = 400$ mM. The improvement for the shorter immersion time (2 h) occurs when $C_0 \geq 500$ mM,

501 which is consistent with the results in Fig. 1(c).

502 The C_0 dependence on η^{F}_{T} can be explained using a two-part hypothesis. First, the
503 cryoprotection from intracellular trehalose of CHO-TRET1 cells increases when the intracellular
504 trehalose starts to saturate. As the intracellular trehalose concentration is undersaturated at $C_0 <$
505 400 mM, the maximum CPA effect from intracellular trehalose occurs at $t = 2$ h. However, as the
506 intracellular trehalose concentration saturates at $t \leq 2$ h when $C_0 \geq 500$ mM, the CPA effect should
507 also saturate at this maximum value. Second, when the intracellular trehalose concentration is
508 undersaturated, the cell mainly takes up trehalose, showing little dehydration. However, after the
509 intracellular trehalose saturates, cell apoptosis progresses before freezing due to excess
510 dehydration. As the uptake rate of trehalose increases with C_0, the intracellular trehalose
511 concentration should reach a maximum at t ≤ 2 h for $C_0 \geq 500$ mM. Then, the apoptosis due to the
512 excess dehydration would significantly decrease the viability in these conditions.

513 Finally, we consider how the freeze–thaw viabilities of CHO-K1 cells depend on the cooling
514 rate H. For CHO-vector cells (Fig. 10(a)), there is little difference between the two immersion times,
515 except when H = 10–30 K/min (corresponding to a freezing temperature of 150–200 K). In this
516 range, the shorter immersion time shows the high viability of 0.4–0.5. According to the results at C_0
517 = 500 mM in Fig. 1(c), the viability of the $t = 2$ h case should be significantly higher than that of 6 h
518 because of the pre-freezing excess dehydration. Therefore, although η^{F}_{V} was almost 0 in the
519 previous study [47] at $t = 6$ h, we found here that the viability becomes high when $H = 10$–30 K/min
520 at $t = 2$ h. This result also shows that the high cryoprotective effect occurs in a remarkably narrow
521 range of H. This result is consistent with the two-factor hypothesis proposed by Mazur *et al.* [28]. If
522 so, this means that the CPA effect of extracellular trehalose for CHO-vector cells is similar to that of
523 other cells.

524 In contrast, for CHO-TRET1 cells, the freezing rate affects the viability roughly equally for
525 both immersion times (Fig. 10(b)). Nevertheless, the cooling rate affects η^{F}_{T}. At the lowest cooling
526 rates $H \leq 10$ K/min, η^{F}_{T} hovers about 0.5, staying relatively low. Then, at middling cooling rates $10 \leq$
527 $H \leq 30$ K/min, the viability η^{F}_{T} reaches a maximum of about 0.75. Then, at the rapid cooling rates of
528 $H \geq 30$ K/min, the viability η^{F}_{T} drops to near 0, even though the apoptosis rate before freezing is

small.

At these higher cooling rates ($H > 30$ K/min), the H dependence on η^{F}_{T} is nearly the same as that on η^{F}_{V}. According to the two-factor hypothesis of Mazur *et al.* [28], suppression of intracellular freezing determines the viability under rapid freezing conditions. Thus, our results indicate that the intracellular trehalose cannot inhibit intracellular freezing at $H \sim 10^2$ K/min conditions. On the other hand, high viabilities are maintained regardless of the cooling rate as long as $H \leq 30$ K/min. This result shows that intracellular trehalose effectively improves the viability of CHO-TRET1 cells for the slow-cooling protocol. Although the two-factor hypothesis of Mazur *et al.* [28] shows that the long-term exposure to a high-concentration solution could reduce the viability in slow cooling, the present study suggests that this effect may be canceled by the uptake of trehalose through TRET1.

Conclusion

To clarify the cryoprotective mechanism of intracellular trehalose on CHO-K1 cells [47], we examined the trehalose uptake characteristics of the CHO-TRET1 cell and its viability. Both CHO-TRET1 cells and CHO-vector cells were simultaneously immersed in a freezing solution containing trehalose at a concentration of 0–1 M for 0–6 hours to prepare each cell sample. The amount of intracellular trehalose was directly measured by HPLC separately from the viability measurements, and both the uptake rate and the total amount of trehalose transported through TRET1 were estimated. The apoptosis rate was also measured to check the cell healthiness during the pre-freezing immersion period. Then, the freeze–thaw viabilities of these cells were measured using the same experimental protocols as in the previous study [47].

As a result, we found that trehalose uptake rate into CHO-TRET1 cells was larger with a higher extracellular concentration C_0, but the intracellular trehalose concentration saturated at C_0 = 400 mM. The upper limit to the amount of intracellular trehalose was about 70–80 pg/cell. Under this saturation condition, the freeze–thaw viability of CHO-TRET1 cells reached about 0.8, their highest value. When $C_0 < 400$ mM, the longer the immersion time, the greater the uptake of

557 trehalose (but less than the maximum value), and the greater the viability. On the other hand,
558 when C_0 > 400 mM, the immersion time for maximum viability became shorter than 2 h. Further
559 immersion would lead to greater apoptosis before freezing, which lowered the freeze–thaw viability.
560 Therefore, our findings suggest that both CHO-vector and CHO-TRET1 cells get stressed by
561 dehydration arising from the osmotic pressure of extracellular trehalose. In the CHO-TRET1 case,
562 this was found to occur after the amount of trehalose in the cell reached saturation.

563 We conclude that the optimum conditions for the cryopreservation of CHO-TRET1 cells
564 with trehalose involve immersion for 2 h in a freezing solution containing C_0 = 400 mM trehalose.
565 We also found that the intracellular trehalose exhibits a CPA effect when the cooling rate is below
566 30 K/min, whereas the extracellular trehalose is only effective as a CPA when the rate lies between
567 10 and 30 K/min.

568

569 **Acknowledgments**

570 This work was partly supported financially by a Grant-in-Aid for Scientific Research from
571 the Japan Society for the Promotion of Science (Grant No. 26105009 and 17K1883407). Trehalose
572 was donated by Hayashibara Co., Ltd. The authors acknowledge the discussion in the Joint
573 Research Program of the Institute of Low Temperature Science, Hokkaido University.

574

575 **References**

576 [1] G.M. Beattie, J.H. Crowe, A.D. Lopez, V. Cirulli, C. Ricordi, A. Hayek, Trehalose: A
577 cryoprotectant that enhances recovery and preserves function of human pancreatic islets after
578 long-term storage, Diabetes 46 (3) (1997) 519–523.
579 [2] N. Chakraborty, M.A. Menze, H. Elmoazzen, H. Vu, M.L. Yarmush, S.C. Hand, M. Toner,
580 Trehalose trasporter from African chironomid larvae improves desiccation tolerance of Chinese
581 hamster ovary cells, Cryobiology 64 (2012), 91–96.
582 [3] T. Chen, A. Fowler, M. Toner, Literature review: Supplemented phase diagram of the
583 trehalose-water binary mixture, Cryobiology 40 (2000), 277–282.
584 [4] J. Crank, The mathematics of diffusion, Oxford Univ. Press, London, (1964) 84–98.

585 [5] J.H. Crowe, L.M. Crowe, J.F. Carpenter, A.S. Rudolph, C.A. Wistrom, B.J. Spargo, T.J.
586 Anchrodoguy, Interactions of sugars with membranes, Biochim. Biophys. Acta 947 (1988) 367–
587 384.
588 [6] J.H. Crowe, L.M. Crowe, Preservation of mammalian cells e learning nature's tricks, Nat.
589 Biotechnol. 18 (2000) 145–146.
590 [7] N. Ekdawi-Sever, J.J. de Pablo, E. Feick, E. von Meerwall, Diffusion of sucrose and α,
591 α-trehalose in aqueous solutions, J. Phys. Chem. A 107 (2003) 936–943.
592 [8] G.D. Elliott, X.-H. Liu, J.L. Cusick, M. Menze, J. Vincent, T. Witt, S. Hand, M. Torner, Trehalose
593 uptake through P2X7 purinergic channels provides dehydration protection, Cryobiology 52
594 (2006) 114–127.
595 [9] A. Eroglu, M.J. Russo, R. Bieganski, A. Fowler, S. Cheley, H. Bayley, M. Toner, Intracellular
596 trehalose improves the survival of cryopreserved mammalian cells, Nature Biotech. 18 (2000)
597 163–167.
598 [10] A. Eroglu, M. Toner, T.L. Toth, Beneficial effect of microinjectioned trehalose on the
599 cryosurvival of human oocytes, Fertil. Steril. 77 (2002) 152–158.
600 [11] A. Eroglu, J.A. Lawitts, M. Toner, T. Toth, Quantitative microinjection of trehalose into mouse
601 oocytes and zygotes, and its effect on development, Cryobiology 46 (2003) 121-134.
602 [12] G.M. Fahy, D.R. MacFarlene, C.A. Angell, H.T. Meryman, Vitrification as an approach to
603 cryopreservation, Cryobiology 21 (1984) 407–426.
604 [13] T. Furuki, T. Ito, N. Asakawa, Y. Inoue, M. Sakurai, Effects of trehalose on the swelling
605 behavior of hydrogel – visualization of the preferential hydration of disaccharides, Chem. Lett.
606 38 (2009) 264–265.
607 [14] C. Gläfke, M. Akhoondi, H. Oldenhof, H. Sieme, W.F. Wolkers, Cryopreservation of Platelets
608 using trehalose: The role of membrane phase behavior during freezing, Biotechnol. Prog. 28 (5)
609 (2012), 1347–1354.
610 [15] T. Gonda, K. Sei, The inhibitory growth mechanism of saccharides on the growth of ice crystals
611 from aqueous solutions, Prog. Cryst. Growth Charact. Mater. 51 (2005) 70–80.
612 [16] N. Guo, I. Puhlev, D.R. Brown, J. Mansbridge, F. Levine, Trehalose expression confers

613 desiccation tolerance on human cells, Nat. Biotechnol. 18 (2000) 168–171.
614 [17] A. Hubel, T.B. Darr, Passive loading of trehalose into cells, Cryobiology 45 (3) (2002) 227.
615 [18] Y. Kanamori, A. Saito, Y. Hagiwara-Komoda, D. Tanaka, K. Mitsumasu, S. Kikuta, M.
616 Watanabe, R. Cornette, T. Kikawada, T. Okuda, The trehalose transporter 1 gene sequence is
617 conserved in insects and encodes proteins with different kinetic properties involved in trehalose
618 import into peripheral tissues, Insect Biochemistry and Molecular Biology 40 (2010) 30–37.
619 [19] A.M. Karow, Jr., O. Carrier, Jr., W.C. Holland, Toxicity of high dimethyl sulfoxide
620 concentrations in rat heart freezing, Cryobiology **3** (6) (1967) 464–468.
621 [20] H. Kawai, M. Sakurai, Y. Inoue, R. Chujo, S. Kobayashi, Hydration of oligosaccharides:
622 anomalous hydration ability of trehalose, Cryobiology 29 (1992) 599–606.
623 [21] M. Kiesel, R. Reuss, J. Endter, D. Zimmermann, H. Zimmermann, R. Shirakashi, E. Bamberg,
624 U. Zimmermann, V. L. Sukhorukov, Swelling-activated pathways in human T-Lymphocytes
625 studied by cell volumetry and electrorotation, Biophysical J. 90 (2006) 4720–4729.
626 [22] T. Kikawada, A. Saito, Y. Kanamori, Y. Nakahara, K. Iwata, D. Tanaka, M. Watanabe, T. Okuda,
627 Trehalose transporter 1, a facilitated and high-capacity trehalose transporter, allows
628 exogeneous trehalose uptake into cells, PNAS 104 (28) (2007) 11585–11590.
629 [23] N. Kimizuka, T. Suzuki, Supercooling Behavior in Aqueous Solutions, J. Phys. Chem. B 111
630 (2007) 2268–2273.
631 [24] A. V. Laere, Trehalose, reserve and/or stress metabolite? FEMS Microbiology Reviews 63 (1989)
632 201–210.
633 [25] C. Lambruschini, A. Relini, A. Ridi, L. Cordone, A. Gliozzi, Trehalose interacts with
634 phospholipid polar heads in Langmuir monolayers, Langmuir 16 (2000) 5467–5470.
635 [26] A. Lawson, H. Ahmad, A. Sambanis, Cryotoxicity effects of cryoprotectants as single-component
636 and cocktail vitrification solutions, Cryobiology 62 (2011) 115–122.
637 [27] P. Mazur, Freezing of living cells: mechanisms and implications, Am. J. Physiol. 247 (1984)
638 C125–C142.
639 [28] P. Mazur, S.P. Leibo, E.H.Y. Chu, A two-factor hypothesis of freezing injury, Experimental Cell
640 Research 71 (1972) 345–355.

641 [29] H. T. Meryman, Cryopreservation of living cells: principles and practice, Transfusion 47 (2007)
642 935–945.
643 [30] K. Mitsumasu, Y. Kanamori, M. Fujita, K. Iwata, D. Tanaka, S. Kikuta, M. Watanabe, R.
644 Cornette, T. Okuda, T. Kikawada, Enzymatic control of anhydrobiosis-related accumulation of
645 trehalose in the sleeping chironomid, *Polypedilum vanderplanki*, FEBS J. 277 (2010) 4215–
646 4228.
647 [31] O. Miyawaki, M. Dozen, K. Hirota, Cooperative hydration effect causes thermal unfolding of
648 proteins and water activity plays a key role in protein stability in solutions, J. Biosci. Bioeng.
649 122 (2016) 203–207.
650 [32] P. O. Montiel, Solubile carbohydrates (trehalose in particular) and cryoprotection in polar biota,
651 Cryo-Lett. 21 (2000) 83–90.
652 [33] J. Motomura, T. Uchida, M. Nagayama, K. Gohara, T. Taira, K. Shimizu, M. Sakai, Effects of
653 additives and cooling rates on cryopreservation process of rat cortical cells, in Physics and
654 Chemistry of Ice (ed. W.F. Kuhs), RSC Publishing, Cambridge, 2007, 409–416.
655 [34] A.E. Oliver, K. Jamil, J.H. Crowe, F. Tablin, Loading human mesenchymal stem cells with
656 trehalose by fluid phase endocytosis, Cell preserv. Technol. 2 (1) (2004) 35–50.
657 [35] C. Polge, A.U. Smith, A.S. Parkes, Revival of Spermatozoa after Vitrification and Dehydration
658 at Low Temperatures, Nature 164 (1949) 666.
659 [36] R. Reuss, J. Ludwig, R. Shirakashi, F. Ehrhart, H. Zimmermann, S. Shchneider, M.M. Weber, U.
660 Zimmermann, H. Shneider, V.L. Sukhorukov, Intracellular delivery of carbohydrates into
661 mammalian cells through swelling-activated pathways, J. Membrane Biol. 200 (1997) 67–81.
662 [37] R. A. Ring, H. V. Danks, The role of trehalose in cold-hardiness and desiccation, Cryo-Lett. 19
663 (1998) 275–282.
664 [38] M.J. Russo, H. Bayley, M. Toner, Reversible permeabilitzation of plasma membranes with and
665 engineered swichable pore, Nature Biotechnol. 15 (1997) 278–282.
666 [39] R. Shirakashi, Saccharide (trehalose) may inhibit intracellular ice formation during freezing,
667 Seisan Kenkyu 55 (2) (2003) 150–152. (in Japanese).
668 [40] R. Shirakashi, C.M. Köstner, K.J. Müller, M. Kürschner, U. Zimmermann, V.L. Sukhrukov,

669 Intracellular delivery of trehalose into mammalian cells by electropermeabilization, J.
670 Membrane Biol. 189 (2002) 45–54.
671 [41] M. Sola-Penna, J. R. Meyer-Fernandes, Stabilization against Thermal Inactivation Promoted
672 by Sugars on Enzyme Structure and Function: Why Is Trehalose More Effective Than Other
673 Sugars? Archives of Biochemistry and Biophysics 360 (1) (1998) 10–14.
674 [42] A.K. Sum, R. Faller, J.J. de Pablo, Molecular simulation study of phospholipids bilayers and
675 insights of the interactions with disaccharides, Biophys. J. 85 (2003) 2830–2844.
676 [43] H. Takahashi, H. Ohmae, I. Hatta, Trehalose-induced destabilization of interdigitated gel
677 phase in dihexadecylphosphatidylcholine, Biophys. J. 73 (1997) 3030–3038.
678 [44] T. Uchida, M. Nagayama, T. Shibayama, K. Gohara, Morphological investigations of disaccharide
679 molecules for growth inhibition of ice crystals, J. Crystal Growth 299 (1) (2007) 125–135.
680 [45] T. Uchida, M. Nagayama, K. Gohara, Trehalose solution viscosity at low temperatures measured by
681 dynamic light scattering method: Trehalose depresses molecular transportation for ice crystal growth, J.
682 Crystal Growth 311 (23-24) (2009) 4747–4752.
683 [46] T. Uchida, S. Takeya, M. Nagayama, K. Gohara, Freezing properties of disaccharide solutions:
684 inhibition of hexagonal ice crystal growth and formation of cubic ice, Crystal Growth, Book 2, InTech –
685 open access pub., Chap. 9, (2012) 203–224.
686 [47] T. Uchida, M. Furukawa, T. Kikawada, K. Yamazaki, K. Gohara, Intracellular trehalose via
687 transporter TRET1 as a method to cryoprotect CHO-K1 cells, Cryobiology 77 (2017) 50–57.
688 [48] T. Uchida, M. Furukawa, T. Kikawada, K. Yamazaki, K. Gohara, Viabilities of long-term
689 cryopreserved CHO-TRET1 cells with trehalose and DMSO, Bull. Glaciol. Res. 37 (2019) 1–9.
690 [49] Z.-W. Yu, P.J. Quinn, Dimethyl sulphoxide: a review of its applications in cell biology, Biosci.
691 Rept. 14 (1994) 259–281.
692 [50] M. Watanabe, T. Kikawada, N. Minagawa, F. Yukuhiro, T. Okuda, Mechanism allowing an
693 insect to survive complete dehydration and extreme temperatures, J. Exp. Bio. 205 (2002)
694 2799–2802.
695 [51] G.R. Wickman, L. Julian, K. Mardilovich, S. Schumacher, J. Munro, N. Rath, S.A.L. Zander, A.
696 Mleczak, D. Sumpton, N. Morrice, W.V. Bienvenut, M.F. Olson, Blebs produced by actin-myosin

contraction during apoptosis release damage-associated molecular pattern proteins before secondary necrosis occurs, Cell Death and Differentiation 20 (2013) 1293–1305.

[52] W.F. Wolkers, N.J. Walker, F. Tablin, J.H. Crowe, Human Platelets loaded with trehalose survive freeze-drying, Cryobiology 42 (2001) 79–87.

[53] M.C. Wusteman, D.E. Pegg, M.P. Robinson, L. Wang, P. Fitch, Vitrification media: toxicity, permeability and dielectric properties, Cryobiology 44 (2002) 24–37.

[54] M.C. Wusteman, D.E. Pegg, L. Wang, M.P. Robinson, Vitrification of ECV304 cell suspensions using solutions containing propane-1,2-diol and trehalose, Cryobiology 46 (2003) 135–145.

[55] M.C. Wusteman, J. Simmonds, D. Vaughan, D.E. Pegg, Vitrification of rabbit tissues with propylene glycol and trehalose, Cryobiology 56 (2008) 62–71.

[56] M. Zhang, H. Oldenhof, H. Sieme, W.F. Wolkers, Freezing-induced uptake of trehalose into mammalian cells facilitates cryopreservation, Biochim. Biophys. Acta 1858 (2016) 1400–1409.

Figure captions

Fig. 1. Freeze–thaw viability η^F vs immersion time t of CHO-vector cells (open symbols) and CHO-TRET1 cells (solid symbols). (a) At the lowest extracellular trehalose-concentration C_0 conditions: 0, 100, and 250 mM. (b) At the intermediate C_0 conditions: 300 and 400 mM. (c) At the highest C_0 conditions: 500 and 1000 mM. Asterisk marks above the symbols of η^F_T mean that there is a significant difference between η^F_T and η^F_V at the same trehalose concentration ($p < 0.01$ by the Tukey–Kramer test). The viability data for 6-h immersion is reproduced from our previous study [47].

Fig. 2. Apoptotic ratios of CHO-vector and CHO-TRET1 cells under various C_0 conditions and immersion times. Bottom of each bar shows the ratio of early apoptosis (A^E). Added white bar on top shows the corresponding ratio of late apoptosis (A^L).

Fig. 3. Time constant K^A of apoptotic ratio at various C_0. K^A_V is for CHO-vector cells and K^A_T is for CHO-TRET1 cells.

Fig. 4. Amount of trehalose taken into CHO-vector cells (M_V) and CHO-TRET1 cells (M_T) vs immersion time t. Extracellular trehalose concentration conditions: 100, 250, 300, 400, 500, 750, and 1000 mM.

Fig. 5. Freeze–thaw viabilities of CHO-vector cells η^F_V and CHO-TRET1 cells η^F_T at immersion time $t \approx 0$ h.

Fig. 6. Time constants K^F_V and K^A_V of CHO-vector cells. K^F_V is from the immersion time dependence on the freeze–thaw viability. K^A_V is from the immersion time dependence on the apoptotic rate.

Fig. 7. Comparison to model of trehalose uptake. C_{in} is the maximum amount of intracellular trehalose measured in the CHO-TRET1 cell. m_{in} is the maximum amount of trehalose expected to inflow into the cell when equilibrated to C_0, assuming no limit for uptake. $(V_0\text{-}\delta V)/V_0$ is the volume change ratio of the cells, owing to dehydration. η^{FT} is the freeze–thaw viability of CHO-TRET1 cells at various C_0 conditions for a 2-h immersion time.

Fig. 8. Apparent transport efficiency Λ into CHO-TRET1 cells. Data based on peak M_t from Fig. 4(b) and Eq. (10). Solid line is the least-square fitting.

Fig. 9. Freeze–thaw viabilities for two immersion times of CHO-vector cells and CHO-TRET1 cells. Asterisk at top marks cases with a significant difference in viabilities between the two times ($p < 0.01$ by the Tukey–Kramer test). The viability data for 6-h immersion is reproduced from our previous study [47].

Fig. 10. Freeze–thaw viabilities for C_0 = 500 mM and various cooling rates H. Two immersion times shown: 2 and 6 h for (a) CHO-vector cells and (b) CHO-TRET1 cells. Asterisk at top marks cases with a significant difference in viability between the two times ($p < 0.01$ by the Tukey–Kramer test). The viability data for 6-h immersion is reproduced from our previous study [47]. The cooling rate is determined from the final temperature target according to the method in [47].

Trehalose uptake and dehydration effects on the cryoprotection of CHO-K1 cells expressing TRET1

(Figure files)

Tsutomu UCHIDA[a*], Maho FURUKAWA[b], Takahiro KIKAWADA[c,d],

Kenji YAMAZAKI[a], and Kazutoshi GOHARA[a]

[a] Division of Applied Physics, Faculty of Engineering, Hokkaido University, N13 W8 Kita-ku, Sapporo, Hokkaido 060-8628, Japan

[b] Division of Applied Physics, Graduate School of Engineering, Hokkaido University, N13 W8 Kita-ku, Sapporo, Hokkaido 060-8628, Japan

[c] Anhydrobiosis Research Group, Institute of Agrobiological Sciences, National Agriculture and Food Research Organization, Ohwashi 1-2, Tsukuba, Ibaraki 305-8634, Japan

[d] Graduate School of Frontier Sciences, The University of Tokyo, 5-1-5, Kashiwanoha, Kashiwa, Chiba 277-8561, Japan

* Corresponding author; e-mail: t-uchida@eng.hokudai.ac.jp; tel&fax: +81-11-706-6635

E-mail address: TU: t-uchida@eng.hokudai.ac.jp

MF: shakiiiiin0a0@gmail.com

TK: kikawada@affrc.go.jp

KY: k-yamazaki@eng.hokudai.ac.jp

KG: gohara@eng.hokudai.ac.jp

Table 1: Symbol definitions and units.

Symbol	Definition	Units
a	average cell diameter	μm
A	apoptosis rate of CHO-vector cell (A_V) and of CHO-TRET1 cell (A_T), further distinguished between early (A^E) and late (A^L) apoptosis	
C_0	extracellular trehalose concentration	mM
C_{in}	intracellular trehalose concentration	mM
C_{out}	initial concentration of the extracellular matrix	mM
D	diffusion coefficient	m^2/s
H	cooling rate	K/min
η^F	freeze–thaw viability of CHO-vector cell ($\eta^F{}_V$) and of CHO-TRET1 cell ($\eta^F{}_T$)	
η^A	apoptotic viability of CHO-vector cell ($\eta^A{}_V$) and of CHO-TRET1 cell ($\eta^A{}_T$)	
K	time constant for the apoptosis rate (K^A) and for the freeze–thaw viability (K^F)	1/h
Λ	apparent transport efficiency	m^2/s
m_{in}	virtual equilibrium intracellular trehalose amount without limit	pg/cell
M	uptake amount of trehalose in CHO-vector cell (M_V) and in CHO-TRET1 cell (M_T)	pg/cell
n_{in}	initial concentration of the extracellular matrix	mol/cell
Π	osmotic pressure under the isotonic condition Π_0, for intracellular Π_{in}, and for extracellular Π_{out}	osmol/kg
R	gas constant	J/mol K
t	immersion time	h
T	temperature	K
V_0	effective volume of average cell	μm^3
δV	amount of dehydration	μm^3

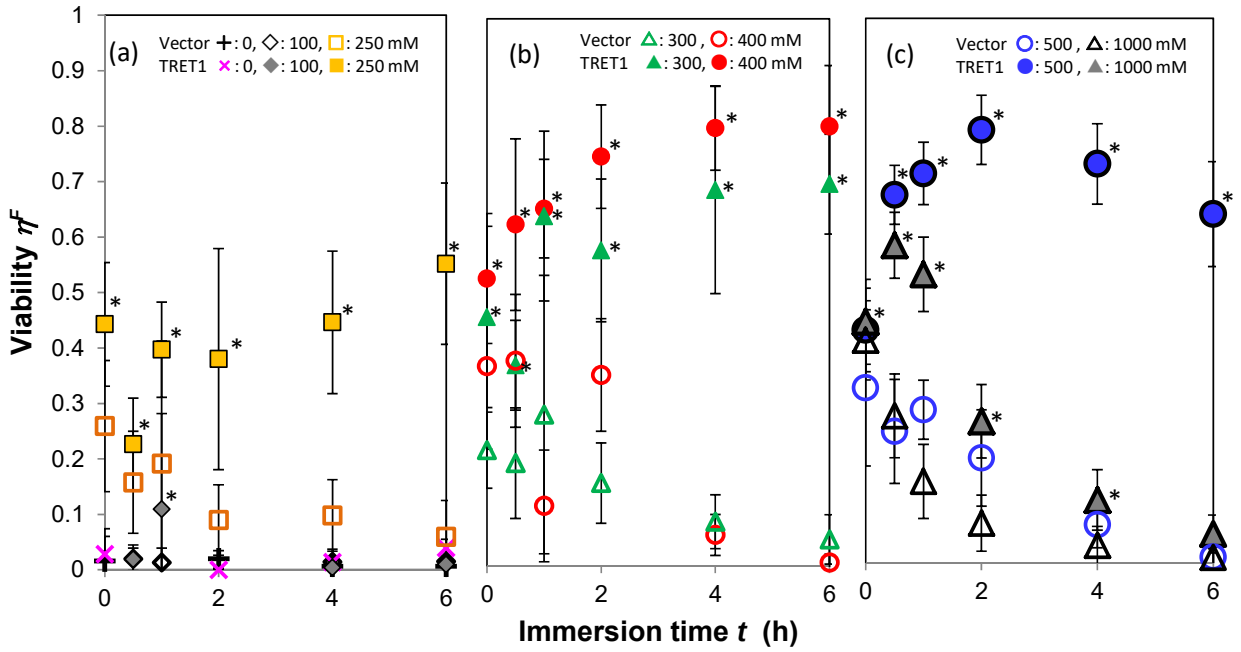

Fig. 1. Freeze–thaw viability η^F vs immersion time t of CHO-vector cells (open symbols) and CHO-TRET1 cells (solid symbols). (a) At the lowest extracellular trehalose-concentration C_0 conditions: 0, 100, and 250 mM. (b) At the intermediate C_0 conditions: 300 and 400 mM. (c) At the highest C_0 conditions: 500 and 1000 mM. Asterisk marks above the symbols of η^{FT} mean that there is a significant difference between η^{FT} and η^{FV} at the same trehalose concentration ($p < 0.01$ by the Tukey–Kramer test). The viability data for 6-h immersion is reproduced from our previous study [47].

Fig. 2

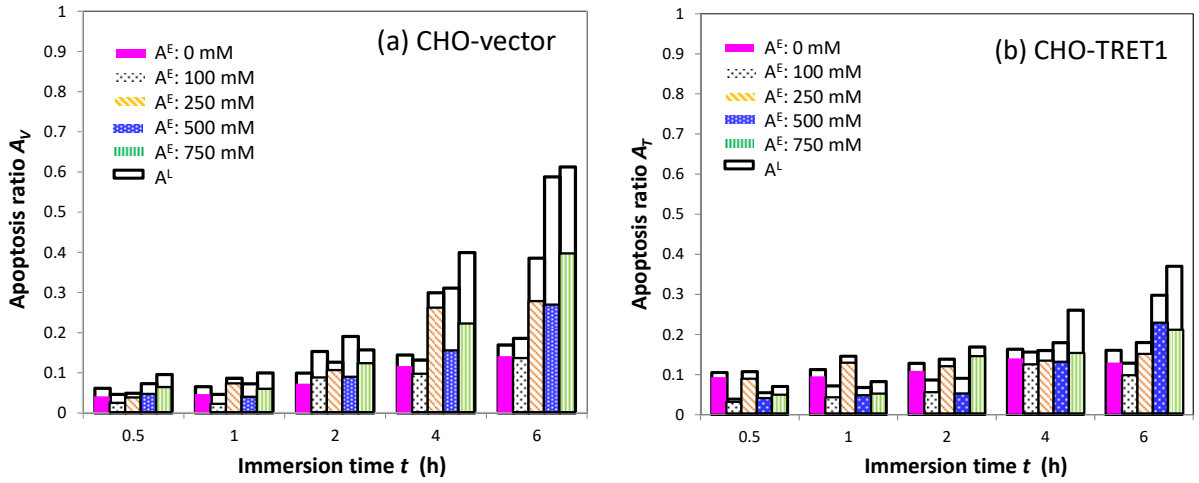

Fig. 2: Apoptotic ratios of CHO-vector and CHO-TRET1 cells under various C_0 conditions and immersion times. Bottom of each bar shows the ratio of early apoptosis (A^E). Added white bar on top shows the corresponding ratio of late apoptosis (A^L).

Fig. 3

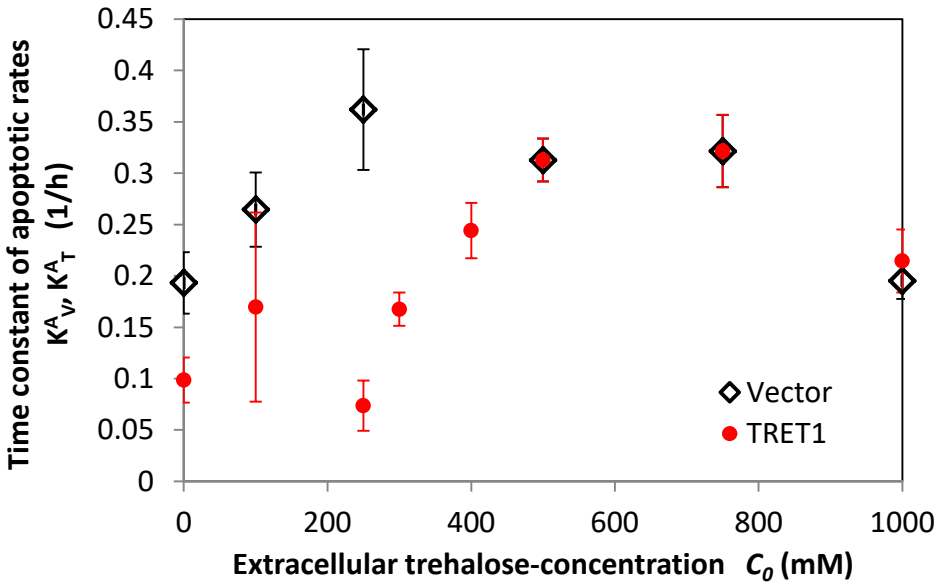

Fig. 3: Time constant K^A of apoptotic ratio at various C_0. K^A_V is for CHO-vector cells for CHO-vector cells and K^A_T is for CHO-TRET1 cells.

Fig. 4

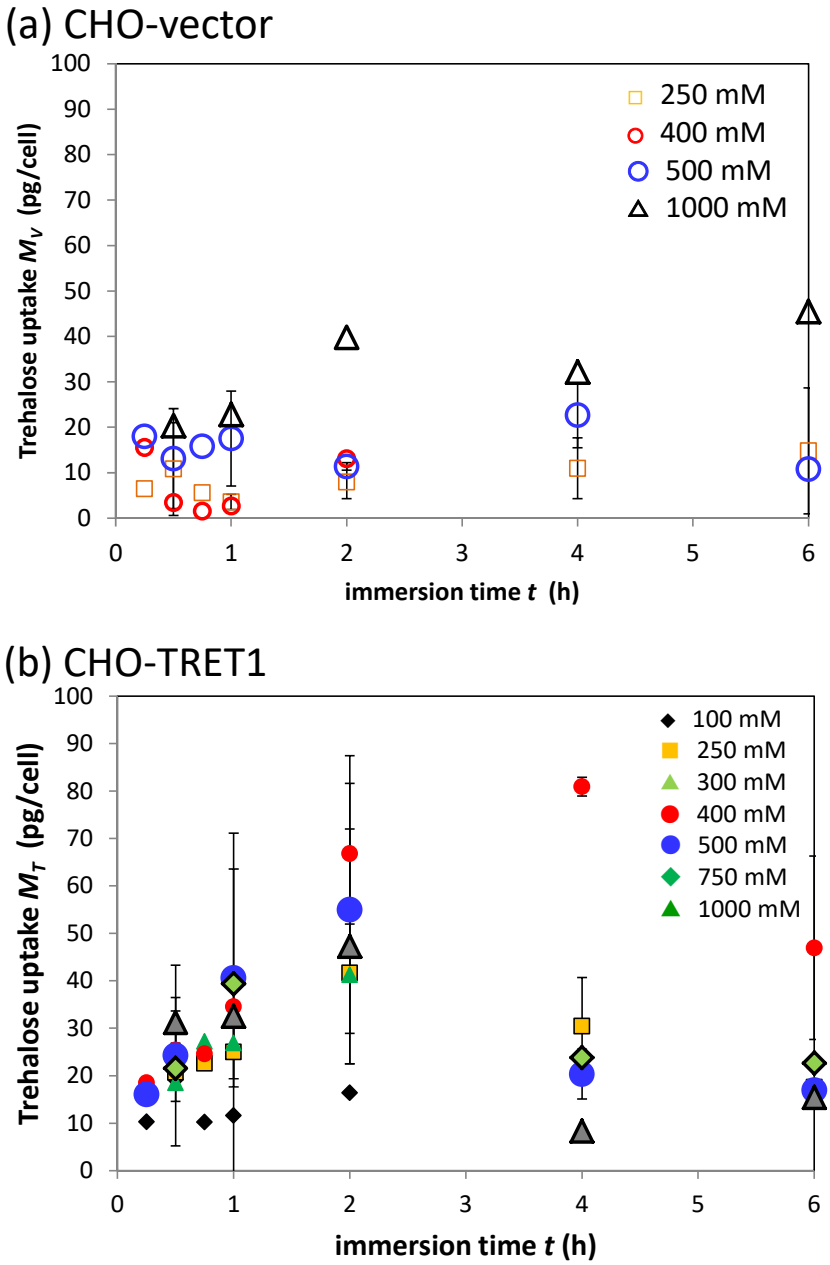

Fig. 4: Amount of trehalose taken into CHO-vector cells (M_V) and CHO-TRET1 cells (M_T) vs immersion time t. Extracellular trehalose concentration conditions: 100, 250, 300, 400, 500, 750, and 1000 mM.

Fig. 5

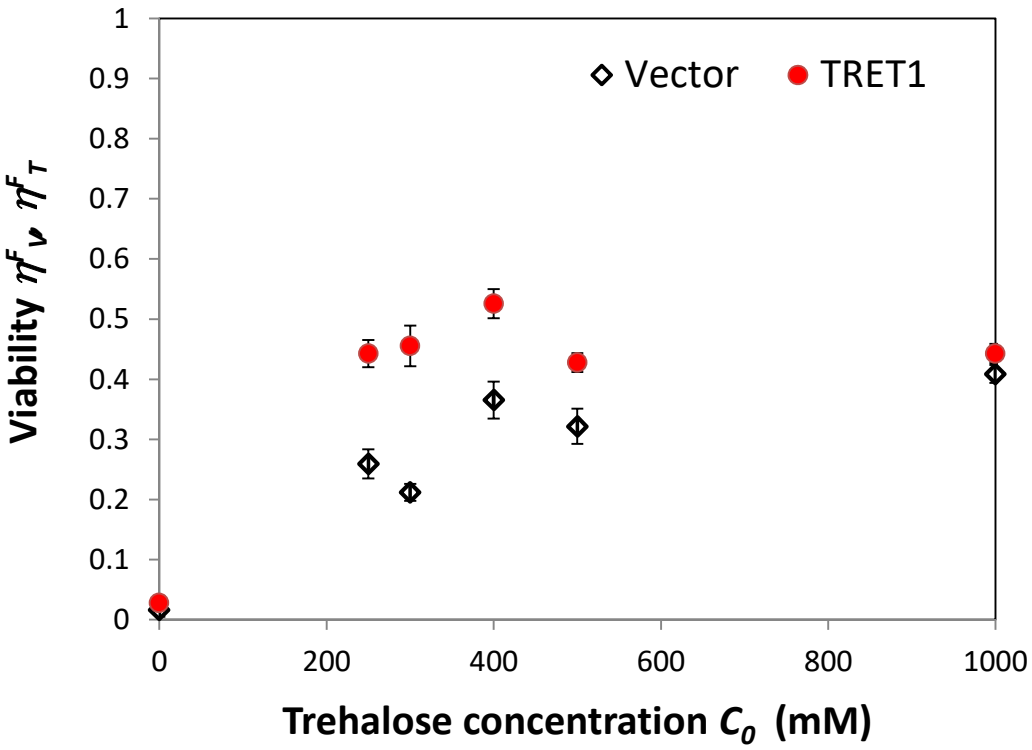

Fig. 5: Freeze–thaw viabilities of CHO-vector cells η^F_V and CHO-TRET1 cells η^F_T at immersion time $t \approx 0$ h.

Fig. 6

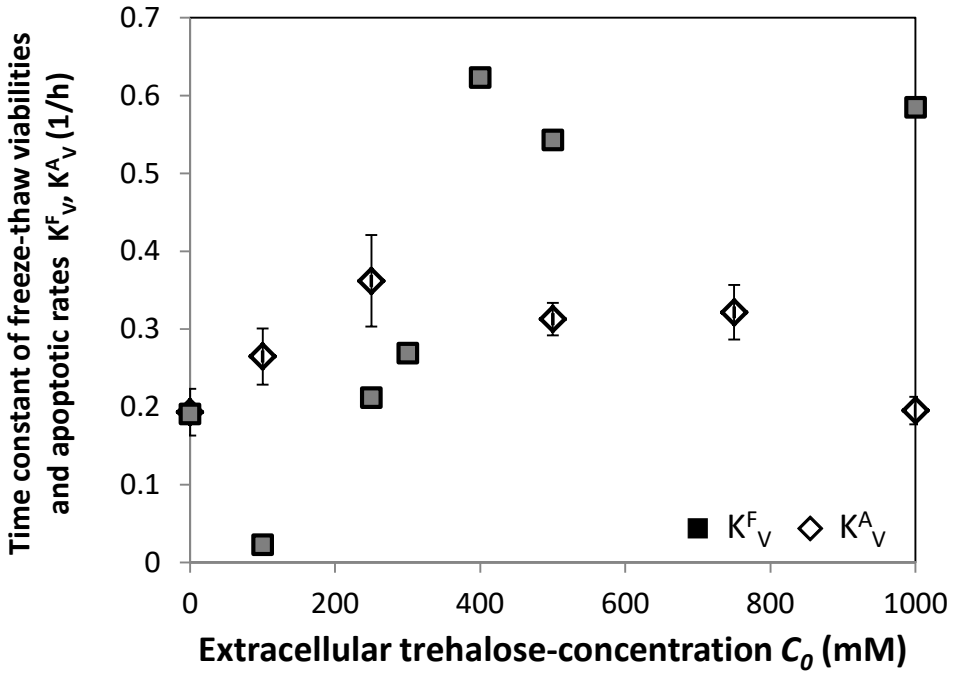

Fig. 6: Time constants K^F_V and K^A_V of CHO-vector cells. K^F_V is from the immersion time dependence on the freeze–thaw viability. K^A_V is from the immersion time dependence on the apoptotic rate.

Fig. 7

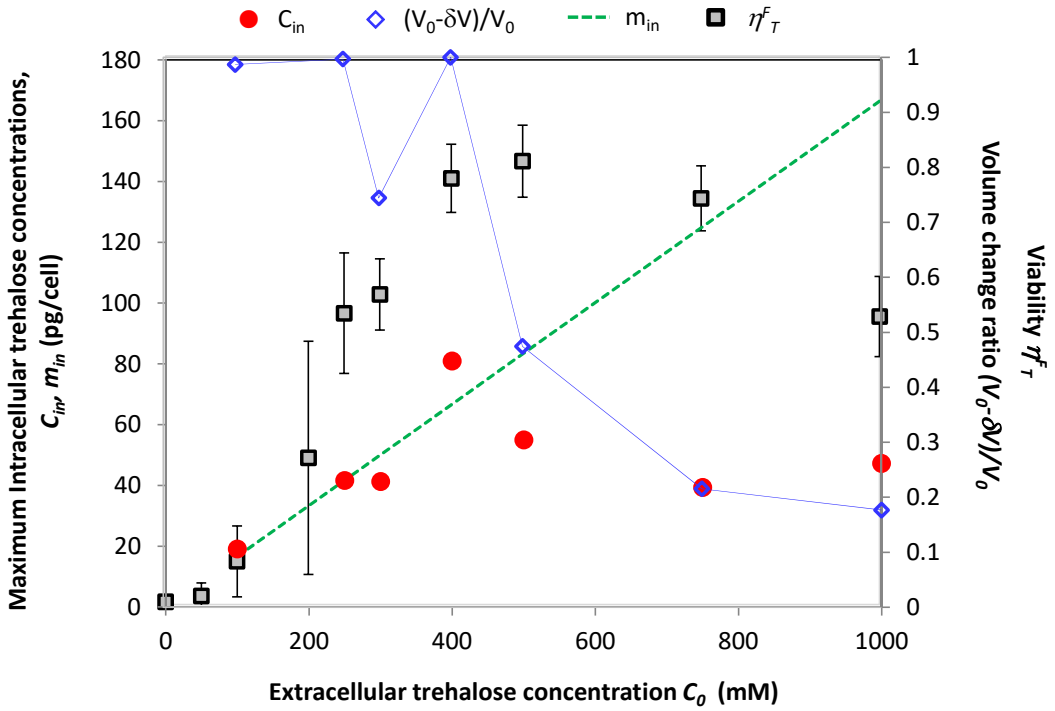

Fig. 7. Comparison to model of trehalose uptake. C_{in} is the maximum amount of intracellular trehalose measured in the CHO-TRET1 cell. m_{in} is the maximum amount of trehalose expected to inflow into the cell when equilibrated to C_0, assuming no limit for uptake. $(V_0-\delta V)/V_0$ is the volume change ratio of the cells, owing to dehydration. $\eta^F{}_T$ is the freeze–thaw viability of CHO-TRET1 cells at various C_0 conditions for a 2-h immersion time.

Fig. 8

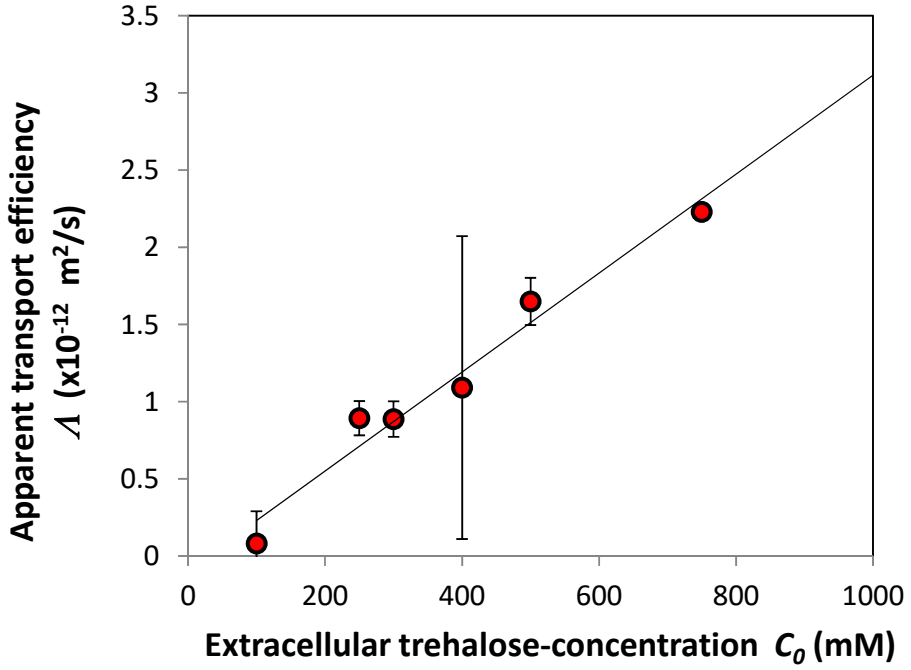

Fig. 8: Apparent transport efficiency Λ into CHO-TRET1 cells. Data based on peak M_t from Fig. 4(b) and Eq. (10). Solid line is the least-square fitting.

Fig. 9

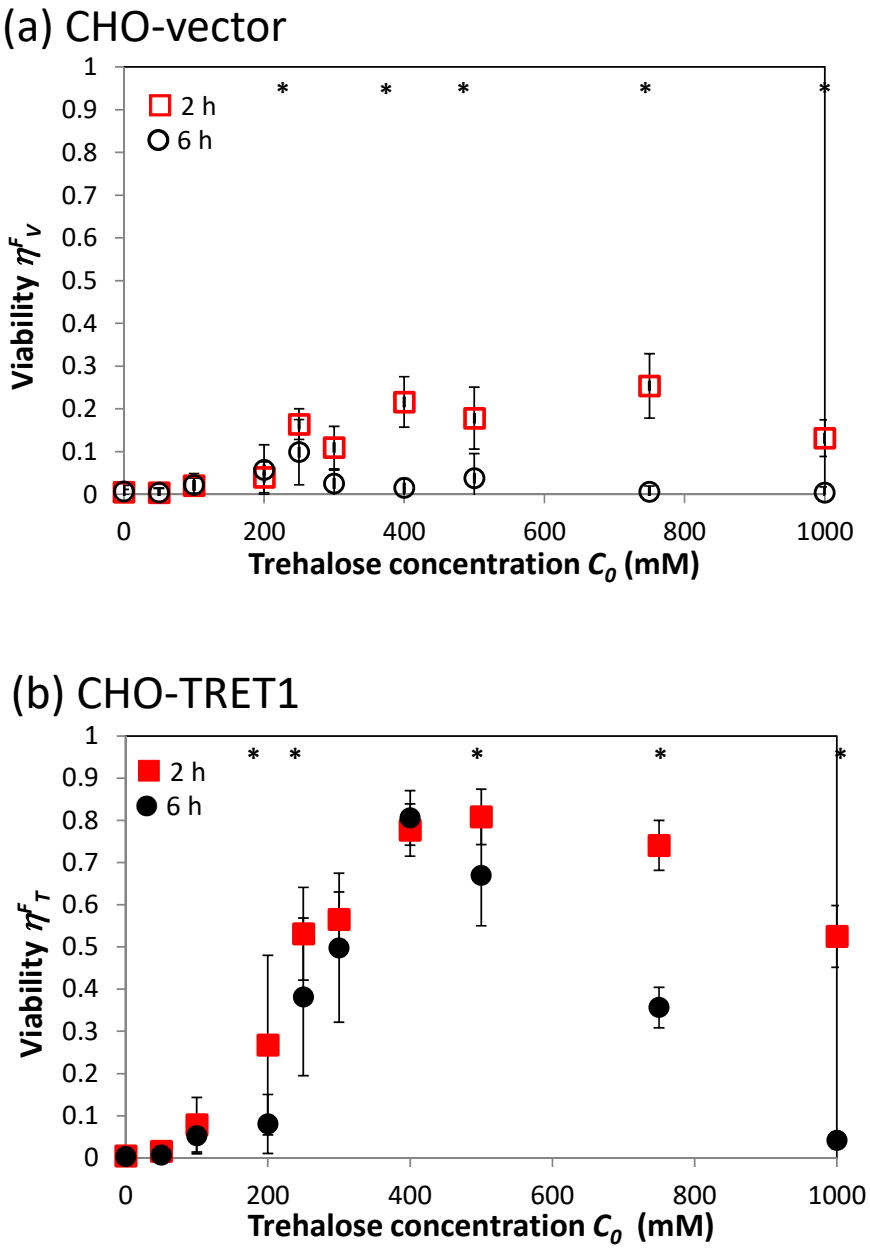

Fig. 9. Freeze–thaw viabilities for two immersion times of CHO-vector cells and CHO-TRET1 cells. Asterisk at top marks cases with a significant difference in viabilities between the two times ($p < 0.01$ by the Tukey–Kramer test). The viability data for 6-h immersion is reproduced from our previous study [47].

Fig. 10

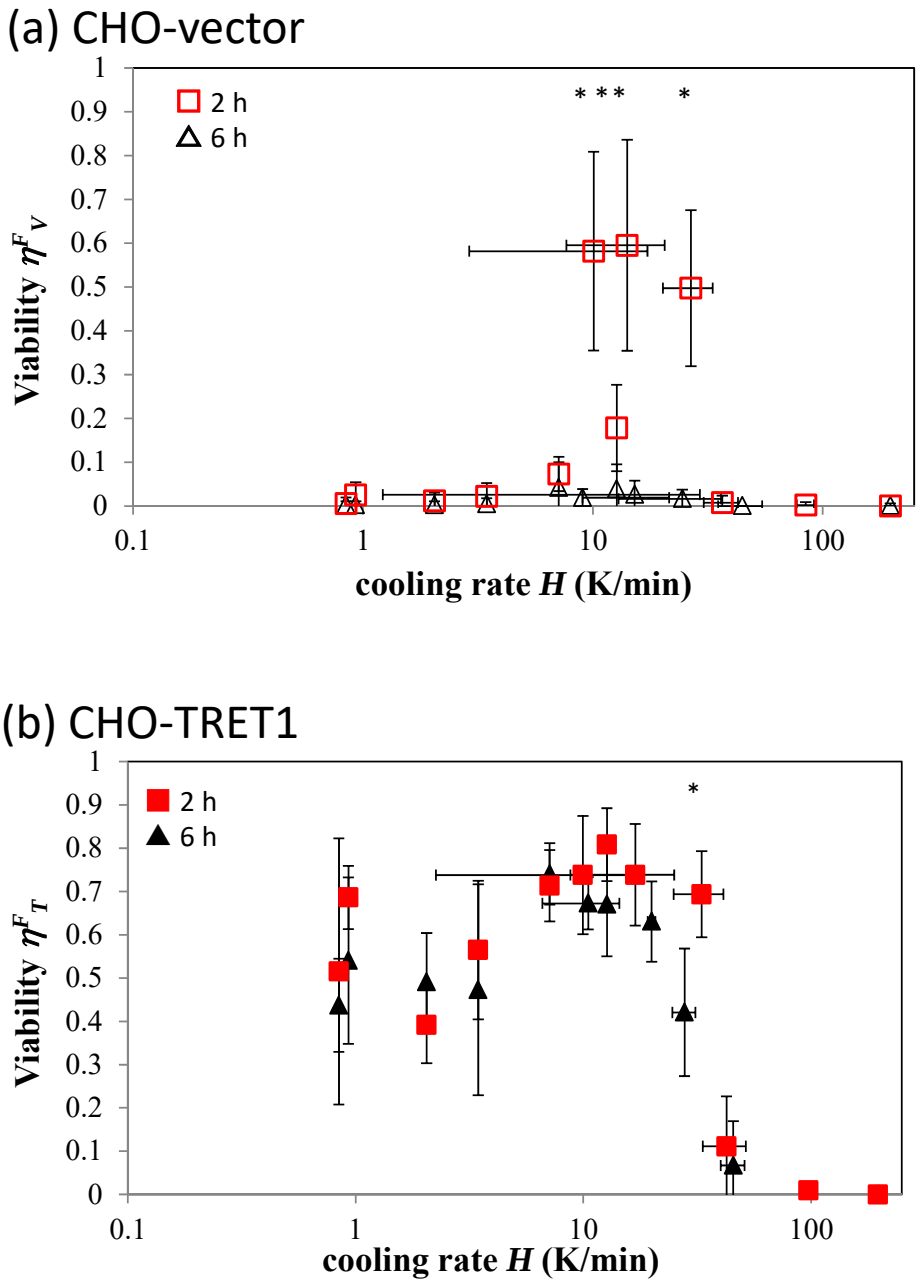

Fig. 10. Freeze–thaw viabilities for C_0 = 500 mM and various cooling rates H. Two immersion times shown: 2 and 6 h for (a) CHO-vector cells and (b) CHO-TRET1 cells. Asterisk at top marks cases with a significant difference in viability between the two times ($p < 0.01$ by the Tukey–Kramer test). The viability data for 6-h immersion is reproduced from our previous study [47]. The cooling rate is determined from the final temperature target according to the method in [47].